Optimizing Pumped Storage Hydro Facility Operation under Uncertainty

Akina Ikudo

Abstract

Unlike water resource management for irrigation purposes, optimizing a hydro facility operation requires the integration of uncertainty in the market price of electricity as well as the uncertainty in the inflow rate. In this research, the framework for a dynamic programming model was established to maximize the expected gross margin from operations. A Markov process was used for the flow rate of water into the reservoirs from streams and the problem was solved for many price scenarios. To reduce the computational effort, a meta-model was constructed for the calculation of the water usage and revenue. Future topics for research are suggested within this study. With these ideas implemented, the model is expected to give desirable operation schedules.

1. Introduction

Planning the operation of a pumped storage hydro facility is subject to various kinds of uncertainty. In the water resource management field, techniques for incorporating the uncertainty in inflows for the multiple reservoirs and relationships between inflows from different rivers have been studied. The work has been summarized in the review article by Labadie (2004). Among the numerous works on the subject, the sampling stochastic dynamic programming approach taken by Kelman et al. (1990) is particularly notable. It employs a scenario based method, overcoming the complexities of representing multi-reservoir operations as a Markov decision process.

Though several optimization methods have been firmly established, the focus was often on meeting demand for irrigation, and therefore, correlations between inflow rates was emphasized. However, when it comes to pumped storage hydro facility, whose primary purpose is to maximize gross margin, hardly any literature was found.

We formulated a dynamic programming model that incorporates the uncertainty in the inflow and the market price of electricity. The scenario based method was used to accommodate price uncertainty, and Markov process was used for the transition of the inflow rate. We estimated the amount of water used and pumped, the revenue, and the cost through the construction of a meta-model. The purpose of this study was to establish a framework for an optimizer that maximizes the gross margin gained by efficiently operating generating and pumping units. The model was to be applied to the Smith Mountain pumped storage hydro facility operated by American Electric Power (AEP). Opportunities for future improvement of the model and its possible use will be explained in the discussion. It is expected that the improved model will provide a robust operation policy under inflow and price uncertainty, and also under an imperfect storm forecast.

2. Model

In this section, the configuration of the system and the model currently used by AEP is explained. Then the changes made to the current model in order to integrate uncertainty are described, followed by the fundamental structure of the dynamic programming model we constructed. Finally, components of the model are described in detail.

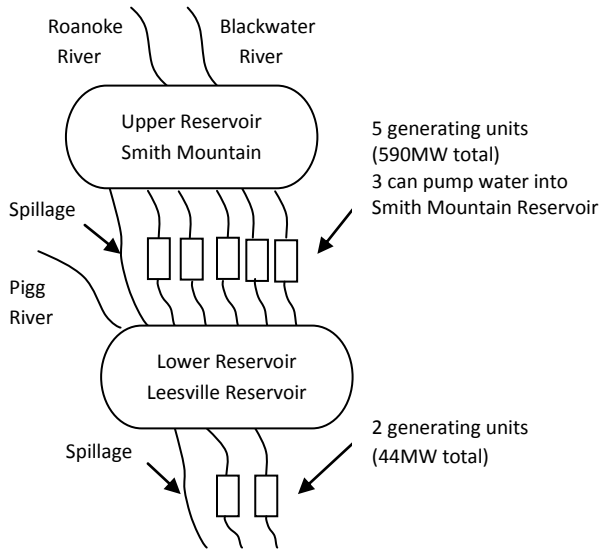

Fig. 1. System Configuration.

2.1 Configuration

The system configuration is shown in Fig. 1. The system consists of two reservoirs; the Smith Mountain reservoir (upper reservoir) and the Leesville reservoir (lower reservoir). Two rivers, Roanoke and Blackwater, flow into the Smith Mountain reservoir, and one river, Pigg, flows into the Leesville reservoir. The water that cannot be stored in the reservoir and is not used for generating, leaves the reservoirs as spillage, S_t^{Smith} and S_t^{Lees}. There are five generating units below the Smith Mountain reservoir, totaling 590MW in generating capacity. Three of these units can pump water back into the Smith Mountain reservoir. There are two small generating units below the Leesville reservoir, which have a total capacity of 44MW.

2.2 Current model

The model currently used by AEP is a deterministic model that uses the forecasted Locational Marginal Price (LMP) at Smith Mountain reservoir, LMP_t^{Smith}, and at the Leesville reservoir, LMP_t^{Lees}. It maximizes the gross margin (GM), a difference between the revenue from generating electricity and the cost of pumping, by changing the amount of generating at the Smith Mountain, $Gen_{i,t}^{Smith}$, generating at the Leesville, $Gen_{j,t}^{Lees}$, and pumping at the Smith Mountain, $Pump_{k,t}$. Index *i*, *j*, and *k* are used to identify the five generating units at the Smith Mountain, the two generating units at the Leesville, and the three pumping units at the Smith Mountain, respectively. The time horizon of two weeks is discretized into one hour intervals, $t \in \{1, \dots, 336\}$. The objective function is expressed as follows:

$$GM = \sum_t \left(\sum_i LMP_t^{Smith} \cdot Gen_{i,t}^{Smith} + \sum_j LMP_t^{Lees} \cdot Gen_{j,t}^{Lees} - \sum_k LMP_t^{Smith} \cdot Pump_{k,t} \right) \quad (1)$$

The amount of generating and pumping is limited by units' capacity:

$$0 \le Gen_{i,t}^{Smith} \le GenMax_i^{Smith} \quad \forall i,t \quad (2)$$

$$0 \le Gen_{j,t}^{Lees} \le GenMax_j^{Lees} \quad \forall j,t \quad (3)$$

$$0 \le Pump_{k,t} \le PumpMax_k \quad \forall k,t \quad (4)$$

In addition, the units at the Smith Mountain are not allowed to generate and pump at the same time:

$$\sum_i Gen_{i,t}^{Smith} \cdot \sum_k Pump_{k,t}^{Smith} = 0 \quad \forall t \quad (5)$$

The volumes of water at Smith Mountain and Leesville reservoir, V_t^{Smith} and V_t^{Lees}, are conserved from one hour to the next hour, and are calculated using the inflow rate forecast, f_t^{Smith} and f_t^{Lees}:

$$V_{t+1}^{Smith} = V_t^{Smith} + C_k \cdot Pump_{k,t} - A_i \cdot Gen_{i,t}^{Smith} + f_t^{Smith} - S_t^{Smith} \quad \forall t \quad (6)$$

$$V_{t+1}^{Lees} = V_t^{Lees} - C_k \cdot Pump_{k,t} + A_i \cdot Gen_{i,t}^{Smith} - B_j \cdot Gen_{j,t}^{Lees} + f_t^{Lees} + S_t^{Smith} - S_t^{Lees} \quad \forall t \quad (7)$$

A_i, B_j, C_k are the conversion factors from MW to ft^3/h for the Smith Mountain generator *i*, the Leesville generator *j*, and the Smith Mountain

pump *k*, respectively. The volumes of the water at the reservoirs have to be within the lower limits, V_{min}^{Smith} and V_{min}^{Lees}, and upper limits, V_{max}^{Smith} and V_{max}^{Lees}, at all time:

$$V_{min}^{Smith} \leq V_t^{Smith} \leq V_{max}^{Smith} \quad \forall t \qquad (8)$$

$$V_{min}^{Lees} \leq V_t^{Lees} \leq V_{max}^{Lees} \quad \forall t \qquad (9)$$

When the lower and upper limits are violated, the units cannot operate. If the five units at the Smith Mountain operate at their capacities, the volume of water in the reservoir drops from the upper limit to the lower limit in 42 hours. Similarly, if the three pumping units at the Smith Mountain operate at their capacities, the volume of the water in the reservoir rises from the lower limit to the upper limit in 114 hours. The storage capacity of the Leesville reservoir is about one third of that of the Smith Mountain, and can be exploited in 68 hours if the two units operate at their capacities. It is reasonable to use 336 hour-, or two-week-, time horizon because the ending volumes of the reservoirs can be adjusted to any levels regardless of the initial volumes.

2.3 Changes made to the model

Several changes were made to the current model in order to incorporate uncertainty in the price and the inflow. The model was reformulated as a dynamic programming, each stage representing one day, instead of one hour. This interval choice was based upon a distinct pattern found in the hourly LMP throughout a day. Fig. 2 shows a typical hourly LMP of a day in February, chosen from the historical data. The LMP stays low during the early morning, reaches the morning peak at 8:00am, gradually declines until 3:00pm, rises to the evening peak at 7:00pm, and declines toward the midnight. This pattern is common in the weekdays in February. Each month has its distinct hourly LMP pattern.

To take advantage of this pattern in the hourly LMP, the idea of a threshold price was introduced. It is intuitive that generating as much electricity as possible when the LMP is high produces

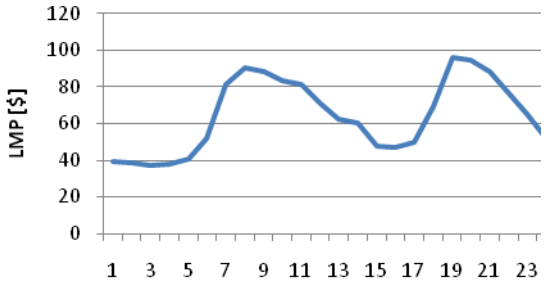

Fig. 2. Hourly LMP in a day.

higher revenue than generating all the time at the low level of generation. Since the amount of water that can be used for generating is limited, there exists a threshold price, above which units generate at their capacities and below which units stay down. The same logic was applied for pumping. When the LMP drops below the threshold price, units pump at their capacity. Though the efficiency of the units for pumping is less than that of generating, the difference in the LMP results in a positive gross margin.

Since the hourly LMP shape is similar from one day to another, it is possible to estimate the amount of water used for generating and pumping when both the average LMP over a day, or daily price index, and the threshold prices are known. Based on this observation, a meta-model that returns the amount of water used for generating, given a daily price index and a threshold price, was constructed. The same principle was applied for the estimation of the amount of water pumped. Using this method, information on hourly water usage was not available, but daily water usage, and therefore the constraints on the reservoir volumes were evaluated at the end of the day, instead of every hour.

2.4 Structure of the dynamic programming model

With threshold prices as decision variables, the dynamic programming model was constructed to maximize the expected gross margin over two weeks. The model consists of fourteen stages, each stage being equivalent to one day. The

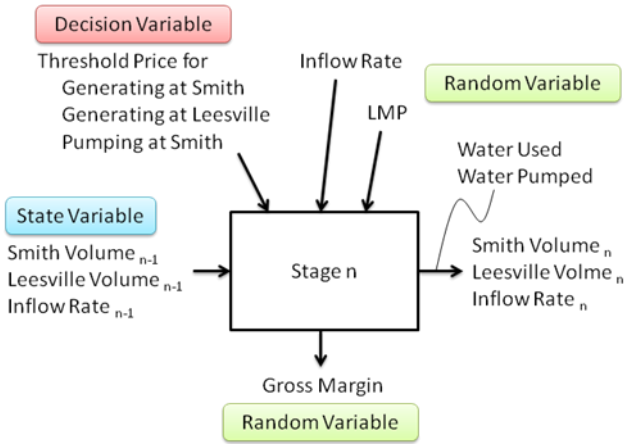

Fig. 3. Dynamic Programming model.

increase in the number of the stages for a long-term operation scheduling can be easily achieved. One stage of the dynamic programming model is illustrated in Fig. 3. To handle with the uncertainty in the LMP, the problem was solved over many two-week long price scenarios. The inflow rate was expressed as distributions based on a Markov process. Thusly, both the amount of water used and pumped and the gross margin could be calculated in a form of expected values in each stage.

The objective function in each stage is a sum of the gross margin from the current stage and the expected gross margin from the next stage to the last stage. It is calculated for each level of the beginning state, and expressed as follows:

$$E[GM]\left(V_{n-1}^{Smith}, V_{n-1}^{Lees}, f_{n-1}^{Smith}\right) = Rev_n^{Smith}\left(P0_n^{Gen\_Smith}, PM_n^{Smith}\right) + Rev_n^{Lees}\left(P0_n^{Gen\_Lees}, PM_n^{Lees}\right) - Cost_n\left(P0_n^{Pump}, PM_n^{Smith}\right) + \sum_{f_n^{Smith}} \left\{ E[GM]\left(V_n^{Smith}\left(f_n^{Smith}\right), V_n^{Lees}\left(f_n^{Smith}\right), f_n^{Smith}\right) \cdot Prob\left(f_{n-1}^{Smith}, f_n^{Smith}\right) \right\} \quad (10)$$

The revenue, Rev_n^{Smith}, Rev_n^{Lees} and the cost $Cost_n$ were calculated using the meta-model, which estimates the revenue and the cost from the threshold price, $P0_n^{Gen\_Smith}$, $P0_n^{Gen\_Lees}$, and $P0_n^{Pump}$, and the average LMP, PM_n^{Smith} and PM_n^{Lees}. The threshold prices are under the following constraints to prohibit the generating and pumping at the same time:

$$P0_n^{Gen\_Smith} \geq P0_n^{Pump} \quad (11)$$

The expected gross margin from the next stage to the last stage was obtained simply by looking up the stored data from the next stage (the "next stage" was actually solved first in the dynamic program). The ending state in each stage depends on the realization of the inflow rate. The distribution of the discretized inflow rate of the current stage is determined by the inflow rate of the previous stage. Multiplying the expected gross margin for each realization of the inflow rate for the current stage by the probability of transitioning from the inflow rate of the previous stage to the inflow rate of the current stage and summing the values up yields the desired expected gross margin. It is worth noting that the inflow rate for the Leesville reservoir does not appear in the equation. This is because the inflow rate of the Leesville is almost proportional to that of the Smith Mountain, and can be calculated by multiplying the inflow rate of the Smith Mountain by some constant, k. The volumes of the reservoirs at the end of each stage are calculated in the following manner and their expected values are constrained by the lower and upper limits:

$$V_n^{Smith}\left(f_n^{Smith}\right) = V_{n-1}^{Smith} + Pump_{k,n}\left(P0_n^{Gen\_Smith}, PM_n^{Smith}\right) - Gen_{i,n}^{Smith}\left(P0_n^{Gen\_Smith}, PM_n^{Smith}\right) + f_n^{Smith} - S_n^{Smith} \quad (12)$$

$$V_n^{Lees}\left(f_n^{Smith}\right) = V_{n-1}^{Lees} - Pump_{k,n}\left(P0_n^{Gen\_Smith}, PM_n^{Smith}\right) + Gen_{i,n}^{Smith}\left(P0_n^{Gen\_Smith}, PM_n^{Smith}\right) - Gen_{j,n}^{Lees}\left(P0_n^{Gen\_Smith}, PM_n^{Smith}\right) + k \cdot f_n^{Lees} + S_n^{Smith} - S_n^{Lees} \quad (13)$$

$$E\left[V_n^{Smith}\right] = \sum_{f_n^{Smith}} \left\{V_n^{Smith}\left(f_n^{Smith}\right) \cdot Prob\left(f_{n-1}^{Smith}, f_n^{Smith}\right)\right\} \quad (14)$$

$$V_{min}^{Smith} \le E\left[V_n^{Smith}\right] \le V_{max}^{Smith} \quad (15)$$

$$E\left[V_n^{Lees}\right] = \sum_{f_n^{Smith}} \left\{V_n^{Lees}\left(f_n^{Smith}\right) \cdot Prob\left(f_{n-1}^{Smith}, f_n^{Smith}\right)\right\} \quad (16)$$

$$V_{min}^{Lees} \le E\left[V_n^{Lees}\right] \le V_{max}^{Lees} \quad (17)$$

If the constraint on the reservoir volume was violated for all the possible values of threshold prices, infeasibility of the problem for the specific beginning state was recorded.

2.5 Components of dynamic programming model

As is mentioned in the above sections, each random variable shown in Fig. 3 was handled in different ways. In this section, the techniques used and the rationale behind them are explained in detail.

2.5.1 Meta-model for water usage and revenue

Since the hourly LMP shapes throughout a day are similar to one another, it is reasonable to estimate the amount of water used and pumped during a day, instead of during each hour. In other words, if the LMP and the threshold price are fixed, the operation schedule should look similar. The inflow rate also affects the water usage, and is implicitly included in the threshold price decision (when the inflow rate is low, a smaller amount of water should be used, which is achieved by setting the threshold price high). The amount of water used is expressed in the number of hours of generation, which can be converted to the amount of water by multiplying it by the maximal water usage rate of the generating units.

The relationships found among the hours of generation, the average LMP for a day, and the threshold price is shown in Fig.4. The graph was plotted using the historical data. Each line represents a certain threshold price. For example, the line at the top with diamond marker shows the number of hours of generation when the threshold price is fixed to \$30. That is, all the generating

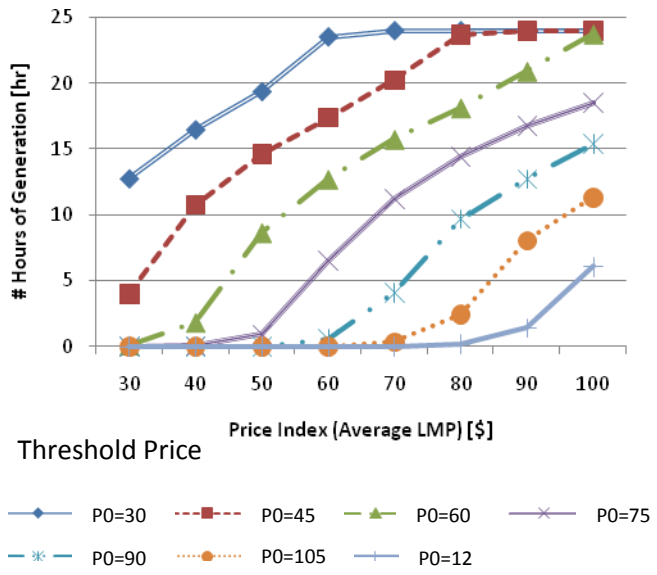

Fig. 4. Relationships among the number of hours of generation, average LMP, and threshold price.

units operate at their capacities when the LMP is above \$30. The horizontal axis is the average price over a day, or the daily price index. As the daily price index increases, the hourly LMP is more likely to exceed the threshold price, and therefore results in a larger number of hours of generation. When the price index is \$100, with threshold prices of \$30, \$45, and \$60, the units are operating 24 hours a day; which means the hourly LMP is above the threshold price throughout a day. On the other hand, when the average LMP is low and the threshold price is high, the units stay down.

The criteria for the regression are 1) when the threshold price is \$0, the number of hours of generation is 24, and 2) when threshold price is \$180, the number of hours of generation is 0. The upper limit for the threshold price, \$180, was obtained by eliminating the higher threshold prices whose effect on the number of hours of generation was not very different from that of \$180 threshold price.

To satisfy the criteria described above and maintain the s-shape of the graph shown in Fig. 4,

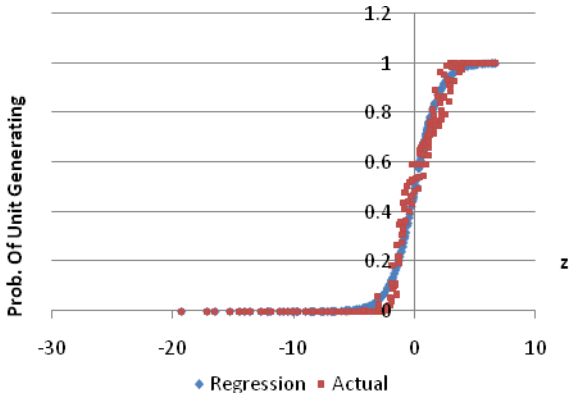

Fig. 5. Logistics regression.

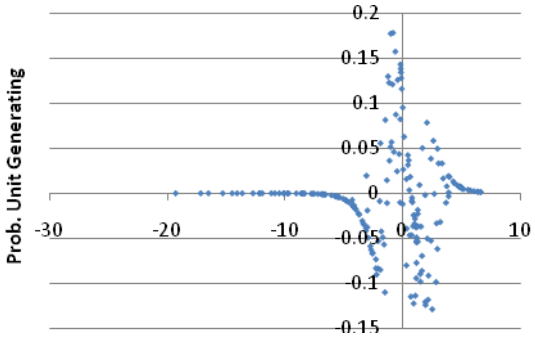

Fig. 6. Residuals of logistics regression.

a logistics regression was chosen as a regression model form:

$$Gen\_hour(Z) = \frac{1}{1+exp(-Z)} \quad (18)$$

$$Z = \alpha_0 + \alpha_1 \cdot P0 + \alpha_2 \cdot PM + \alpha_3 \cdot P0 \cdot PM + \alpha_4 \cdot P0^2 + \alpha_5 \cdot PM^2 + \alpha_6 \cdot P0^3 + \alpha_7 \cdot PM \quad (19)$$

$Gen\_hour(Z)$ gives a fraction of the time the units are generating. The regression and the actual observations are shown in Fig. 5. Though relatively large deviations from the regression was observed around Z=0, which is more explicitly shown in Fig. 6, the regression was fitted fairly well. When the residual was converted to the volume of water and plotted against the amount of water used, a certain pattern was observed (Fig. 7); however, as the histogram of the residuals in Fig. 8 indicates, the residuals center around 0, most of them being relatively small.

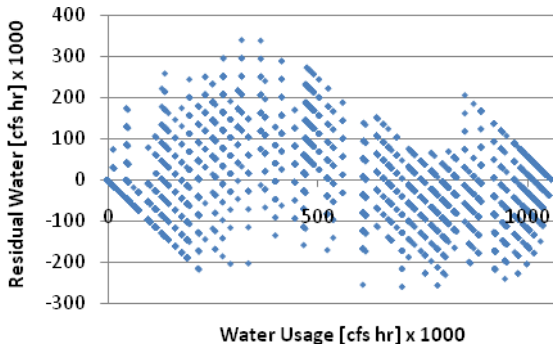

Fig. 7. Residuals in volume of water plotted against amount of water used.

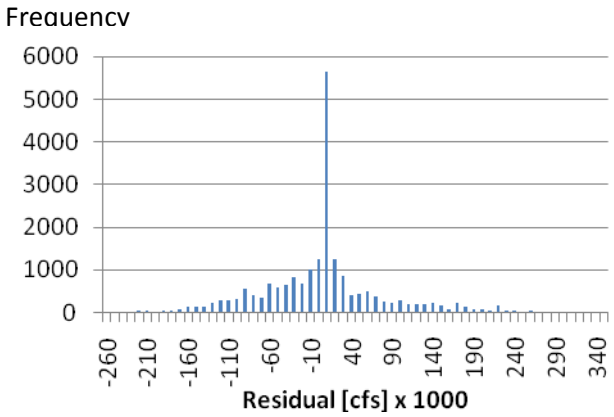

Fig. 8. Histogram of residuals of logistics regression.

Using the following equation, the number of hours of generation was converted to the volume of water:

$$Gen(P0, PM) = 24 \cdot Gen\_hour(P0, PM) \cdot GenMax \quad (20)$$

The same logic and the regression model form were used for the amount of water pumped.

The relationship among the revenue, price index, and threshold price (Fig. 9) was similar to that of the number of hours of generation, price index, and threshold price. Since the revenue is directly related to the amount of water used, and the quadratic term of the threshold price and average LMP are already included in the regression of water usage, a linear regression model was assumed and applied for the revenue.

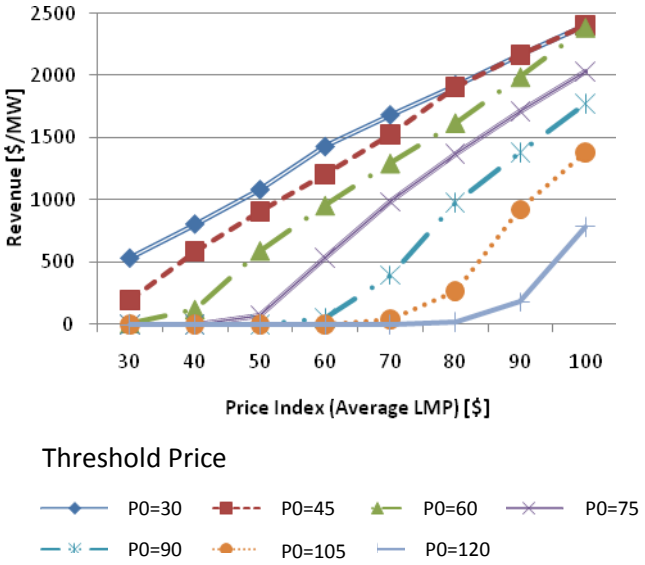

Fig. 9. Relationship among revenue, average LMP, and threshold price

Since the elimination of the threshold price term did not affect the residuals, it was eliminated from the regression model form and the final form was obtained:

$$Rev(P0, PM) = \beta_1 \cdot PM + \beta_2 \cdot Gen\_hour(P0, PM) \quad (21)$$

The constant term was dropped because the better regression was obtained without it. The resulting regression yielded $R^2 \approx 0.9$. The criterion for the revenue regression is that when the number of hours of generation is zero, the revenue goes to zero. However, the regression model shown above does not satisfy this condition. To solve this problem, the optimizer forced the revenue to be zero when the number of hours of generation was zero. The error caused by this modification was negligible since β_1 was about 0.6 whereas β_2 was about 40, indicating that the effect of the average price was much less compared to that of the number of hours of generation.

One thing that needs to be mentioned is that the meta-model, or regression, was constructed for each month. As is mentioned in the section above, the hourly LMP shape throughout a day differs from month to month. The hourly LMP

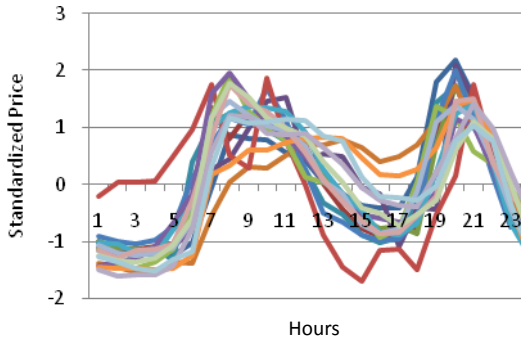

Fig. 10a. Hourly LMP shape of Mondays in March.

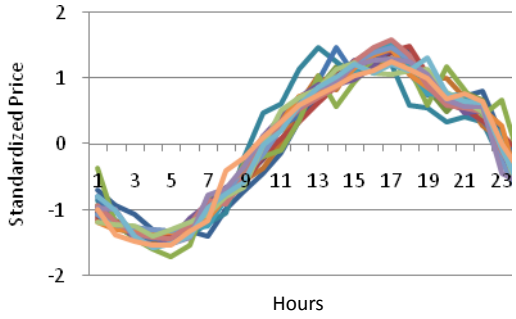

Fig. 10b. Hourly LMP shape of Mondays in July.

shape for Mondays in March and July are shown in Fig.10a and b. To compare the hourly LMP with different averages, the hourly LMP was standardized in the following way:

$$Standardize\ Price = \frac{LMP - Average\ LMP\ (over\ a\ day)}{Standard\ Deviation\ (over\ a\ day)} \quad (22)$$

When compared within a month, the hourly LMP shape of Sundays was distinguishable from that of the other days of the week. The comparison between Mondays and Sundays in April is shown in Fig. 11a and b. Though whether or not the hourly LMP shape of Sundays differs from that of the other days of the week relies on, to some extent, a subjective judgment, the clustering shown in Fig. 12 indicates that the Sunday shape is somewhat different from the others. The LMP at 12:00am, 4:00am, 8:00am, 4:00pm, and

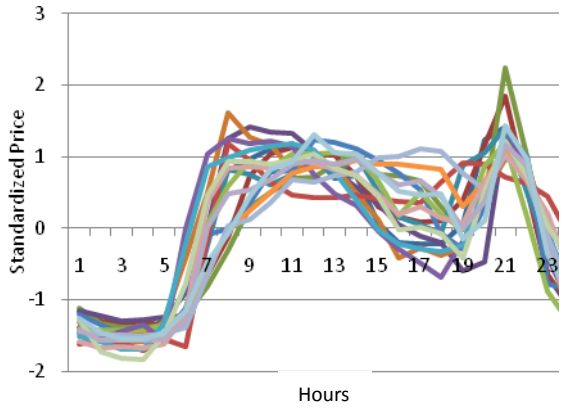

Fig. 11a. Hourly LMP shape of Mondays in April.

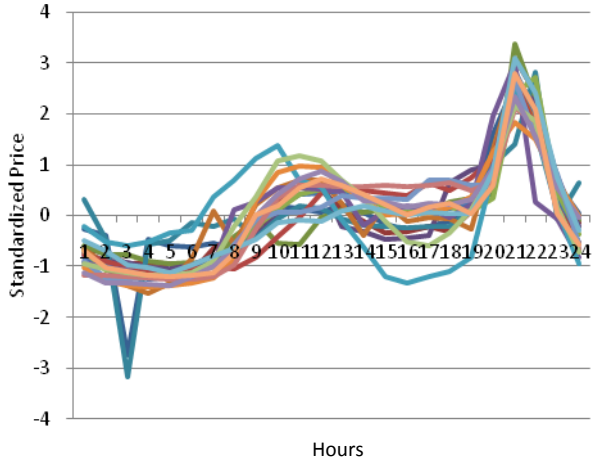

Fig. 11b. Hourly LMP shape of Sundays in April.

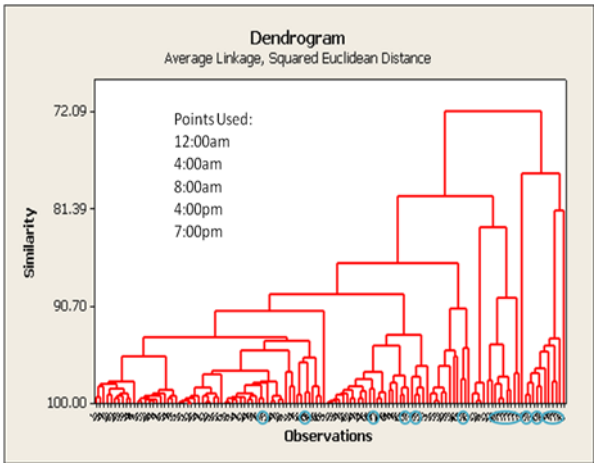

Fig. 12. Clustering of hourly LMP shapes

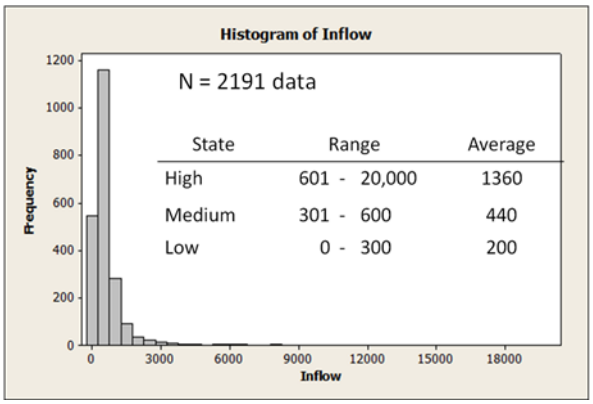

Fig. 13. Histogram of historical inflow rate.

7:00pm were used for clustering. The blue circles represent Sundays. Many of Sunday shapes appeared close to the right end.

2.5.2 Markov process of inflow rate

Since the Markov process has often been used in past studies and gives a realistic inflow rate change, it was applied to our model. The discretization of the inflow rate was less likely to cause problems because the inflow rate is small compared to the amount of water used for generating. Two thirds of the historical inflow rate falls below 600 ft^3/s, whereas the generating units use water at a rate of 44,000 ft^3/s. Since the peaks of all the three inflows, two into the Smith Mountain reservoir and one into the Leesville reservoir, were almost synchronized, the inflow into the upper reservoir, Roanoke and Blackwater were combined, and the inflow into the lower reservoir, Pigg was calculated by multiplying the combined inflow to the upper reservoir by a constant. The historical inflow rate, Roanoke and Blackwater combined, ranged from 80 to 20,000 ft^3/s. The histogram is shown in Fig.13. To reduce the computational effort, all of the inflow rates in the history were discretized into three levels. The discretization was done in a way such that all states contain the same number of historical data. The value for each state is set to the average value of the group. For example, the inflow rates of 601-20,000 ft^3/s were categorized into the state "High", and contains one third of

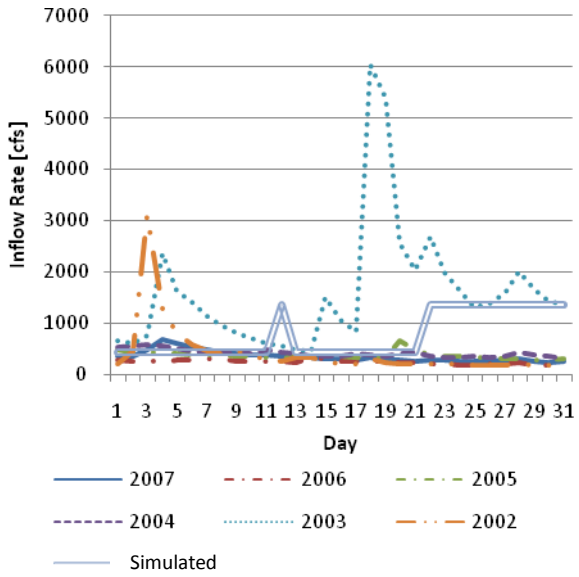

Fig. 14. Inflow rate in May simulated using Markov process.

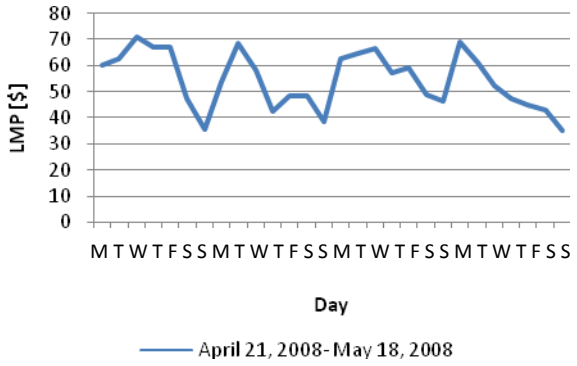

Fig. 15. Weekly LMP pattern.

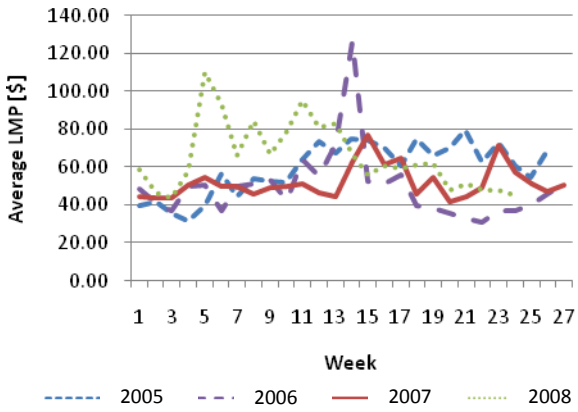

Fig. 16. Weekly price indices.

the historical data. The value 1,360 ft^3/s is the average inflow rate of the data categorized into this state. It is worth noting that the transition matrix for the wet season (May-October) was made separately from the dry season (November-April) to accommodate the difference in seasonal behavior of the rivers. The forecast can be integrated in the scheme simply by changing the probability of transitioning from one state to another. The simulated inflow rate change along with the historical data is shown in Fig.14.

2.5.3 Price scenario/shape simulator

Unlike the inflow rate, the price change cannot be easily expressed as a Markov process because the dependency of the price of today on the prices of the past is strong but estimating today's price by only considering yesterday's price may result in an unrealistic price change when observed in the long term. This is depicted in Fig.15. The graph shows a change in daily price index for four weeks. In general, weekends have a lower LMP, resulting in distinct weekly pattern. To keep this pattern, a week-long daily index price was treated as a set. Though other forecasting methods could have been used, assuming no radical change in the average price or the weekly LMP shape, the criteria for price scenario/shape simulator was set to generate scenarios/shapes that mimic the historical data. It is worth noting that the simulator can be easily replaced by any forecasting methods if preferable.

When the average LMPs over a week, or the weekly price indices, are plotted for seven months, from May to October, the graph in Fig.16 is obtained. The differences between all the pairs of adjacent two points, within a same year, were then calculated and plotted in the histogram shown in Fig.17. The purpose of this analysis was to obtain the typical difference in weekly price indices. Though the sample mean and standard deviation of the data were 0.25 and 14.5,

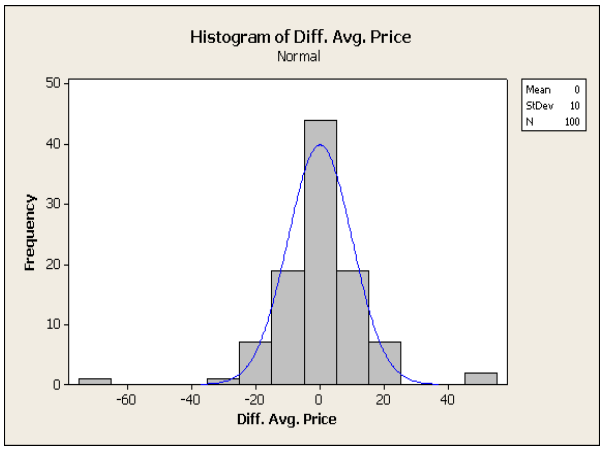

Fig. 17. Histogram of differences in weekly price indices.

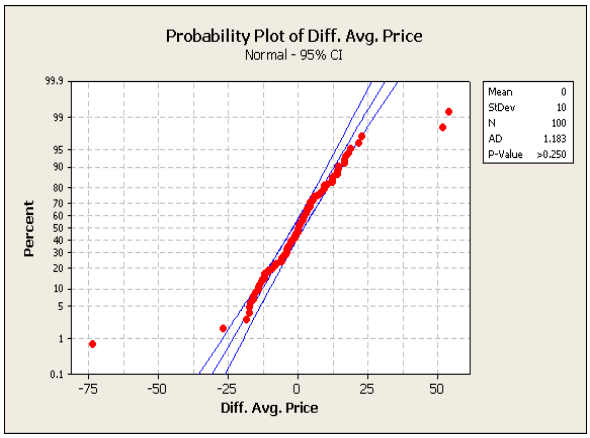

Fig. 18. Probability plot of differences in weekly price indices.

respectively, they were modified to obtain a better Normal distribution fit. With the modified mean of 0 and standard deviation of 10, a p-value over 0.25 was obtained. The probability plot is shown in Fig.18. Though the p-value is not considerably large, when the existence of the outliers was taken into account, it was reasonable to assume Normal distribution.

The shift in the average of the weekly price indices was then analyzed. The average LMPs over a month, or monthly price indices and weekly price indices, are plotted together in Fig.19. The weekly price indices are plotted only from May through October. When they are seen as "noise", the change in the average weekly price indices can be observed as a change in monthly price indices. The differences in the monthly price indices, which are equivalent to the differences in the averages of the weekly price indices over four weeks, when divided by four weeks, turned out to have a mean of zero, and a standard deviation of 3.4. The histogram indicated that the distribution was fairly Normal. However, when Normal distribution was used for both the change in the average of the weekly price indices and the difference in the weekly price indices, unusual gaps in the weekly price indices were observed. To prevent this from happening, the weekly price index was determined to be calculated as followings:

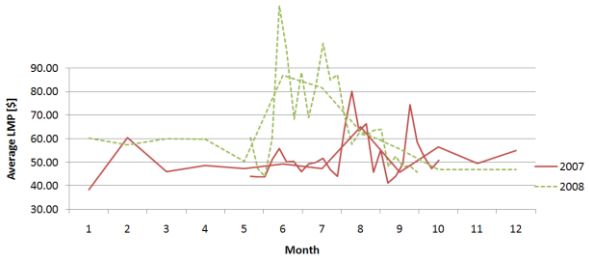

Fig. 19. Weekly price indices and monthly price indices.

$$PI_{n'}^{wk} = PI_{n'-1}^{wk} + 3.4 \cdot \lambda + Normal(0,10)$$

$$\lambda = \{-1,0,1\} \qquad (23)$$

The first term is the weekly price index of the previous week. 3.4 is the standard deviation of the differences in the averages of the weekly price indices. The probability of realizing each value of λ was given to the optimizer as an input, allowing the user to incorporate the price forecast. The values of the last term come from the Normal distribution with the mean of zero and the standard deviation of 10, which represents the variability in the week-to-week price index change. Finally, the weekly price index is converted to the daily price index:

$$PI_n^{dy} = \mu \cdot PI_{n'}^{wk},\ \mu = \frac{PI_n^{dy}}{PI_{n'}^{wk}} \qquad (24)$$

The conversion factor from the weekly price index to the daily price index, μ, is a vector with seven elements and is calculated using the one-week long LMP in the historical data. With this method, the LMP pattern over a week, mentioned at the beginning of this section, was maintained. Fig. 20a shows the daily price indices for two weeks, generated by the simulator. The weekly price index of $50 was used as the weekly price index of the previous week. It mimics the historical price indices shown in Fig.20b.

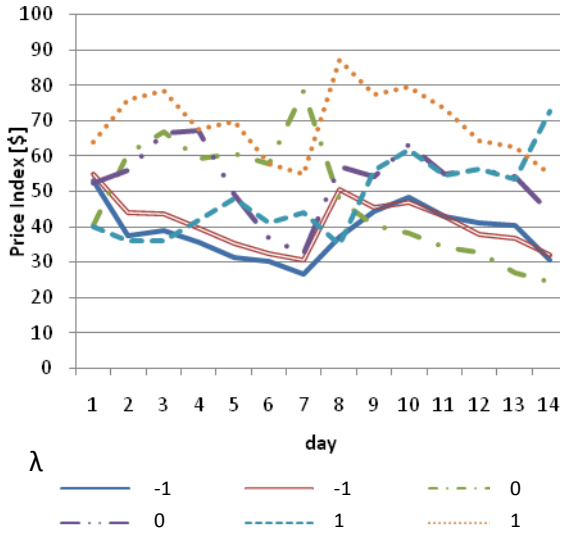

Fig. 20a. Generated price by a simulator.

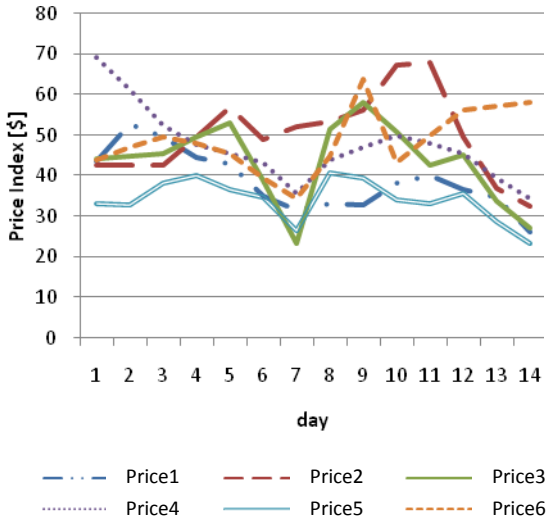

Fig. 20b. Prices from the historical data.

3. Result and discussion

The total enumeration was used for the search of the optimal threshold prices, with a step of $5. Each state variable was discretized into three states, totaling 27 possible states, and optimized for two weeks, using 10 price scenarios. The problem was solved in 37 minutes by excel, using Intel® Core™ 2CPU, 6600@2.4GHz, 2GB of RAM.

For future research, the efficient search of the solution at each stage will be investigated. This will enable the optimizer to have more levels of state variables, and also solve for more price scenarios/shapes. The meta-model for estimating the amount of water used and pumped, the revenue, and the cost will be also refined. Finally, the operating head will be taken into account to accurately estimate the amount of water pumped. By closely looking into the hour by hour operation, it will be expected that the possible violation of the reservoir volume, which may exist in the presented model, will be prevented.

4. Conclusion

This paper has suggested and described a dynamic programming approach to the optimization of the pumped storage hydro facility operation. By introducing the idea of a threshold price, the water used and pumped, the revenue, and the cost were able to be regressed against the market price and the threshold price, evaluating the constraint at the end of each day. To accommodate the inflow rate uncertainty, a Markov process was used, and the fourteen-day optimization problem was solved over many price scenarios/shapes that mimic the historical data. With the improvement on the method of the solution search, regression, and the integration of operating head effect, the model is expected to give a more reliable solution that takes the uncertainty in the inflow rate and the price into account.

Acknowledgement

I would like to express my appreciation to my advisor, Dr. Clark. A. Mount-Campbell, for his guidance and support throughout the project; and Dave Dippold, for providing data and warm encouragement.

References

Kelman, J., Stedinger, J., Cooper, L., Hsu, E., and Yuan, S.-Q. (1990). "Sampling stochastic dynamic programming applied to reservoir operation." Water Resource Research, 26(3), 447-454.

Labadie, M. (2004). "Optimal operation of multireservoir systems: state-of-the-art review." Journal of Water Resources Planning and Management, 130(2), 93-111.